THE BELL SYSTEM TECHNICAL JOURNAL
Vol. 55, No. 10, December 1976
Printed in U.S.A.

Scattering and Absorption Losses of Multimode Optical Fibers and Fiber Lasers

By D. MARCUSE

(Manuscript received May 24, 1976)

We present an approximate theory of loss coefficients for modes of step-index fibers with various types of distortions and for fibers with lossy claddings. The fiber irregularities are assumed to be sinusoidal and random variations of the core-cladding interface. Formulas for the loss coefficients are presented and plotted for different values of the compound mode number M. For fiber lasers, we plot the loss coefficients as functions of the mirror tilt angles.

We consider as an example a Nd-YAG fiber laser with refractive index $n_1 = 1.8$ and a core radius of $a = 40$ μm operating at a wavelength of $\lambda = 1.06$ μm. For this example, we find that radiation losses are caused by Fourier components of fiber irregularities in the spatial wavelength range between 0.4 and 1.3 μm. Intrinsic losses may be as low as $2\alpha = 10^{-3}$ cm^{-1}. It is thus desirable to limit scattering losses to values below 10^{-3} cm^{-1}. This requirement imposes tolerance restrictions of 0.01 μm on the permissible core radius fluctuations. For core radius fluctuations of this order of magnitude, mirror tilts should not exceed approximately 5 degrees. Cladding losses are not critical, but their influence on laser losses depends on the refractive index ratio of the core and cladding materials. Tolerable cladding losses may range from 10 to 300 cm^{-1}.

I. INTRODUCTION

A cavity laser consists of an active medium that provides the required gain and a (usually open) external cavity furnishing the feedback for laser operation. A fiber laser also has gain and feedback, but instead of using the resonant modes of an open cavity it employs an optical fiber for guiding the radiation back and forth between the set of mirrors forming the cavity.[1,2] A fiber laser thus might be much narrower than a cavity laser since it need not allow space for the diffraction-limited beam to spread out in transverse direction. The width of the fiber laser is limited only by the loss of the fiber waveguide, which increases with decreasing fiber diameter.

In this paper we calculate the mode losses of step-index fibers and use them to estimate the losses of fiber lasers. The losses are caused by scattering from the rough fiber wall and by the presence of a lossy cladding. Figure 1 shows a schematic of the fiber laser. We assume that plane mirrors are placed at the end of the fiber that also contains the gain mechanism for the laser. Figure 1a shows a fiber laser with plane mirrors positioned exactly perpendicular to the fiber axis, whereas Fig. 1b shows a laser with slightly tilted mirrors so that the wave inside the fiber, indicated schematically by a light ray, interacts more strongly with the fiber wall. For simplicity, we assume that the mirrors and the medium inside the fiber do not cause scattering and that only the fiber walls are slightly rough. We also assume that the fiber is surrounded by a lossy cladding that causes power loss via the evanescent field tail of the guided wave penetrating into the cladding. However, we consider these various loss mechanisms separately, one at a time.

It is important to realize that wall roughness or other geometrical imperfections of the fiber geometry or inhomogeneities in the fiber material do not necessarily cause resonator losses. The electromagnetic field inside the cavity adjusts itself to any geometry and forms a normal mode. This normal mode of the cavity can be described as a superposition of coupled modes of the perfect waveguide. Henceforth, we shall refer to modes of the perfect structure as ideal modes or as perfect modes. The fiber imperfections provide the mechanism that

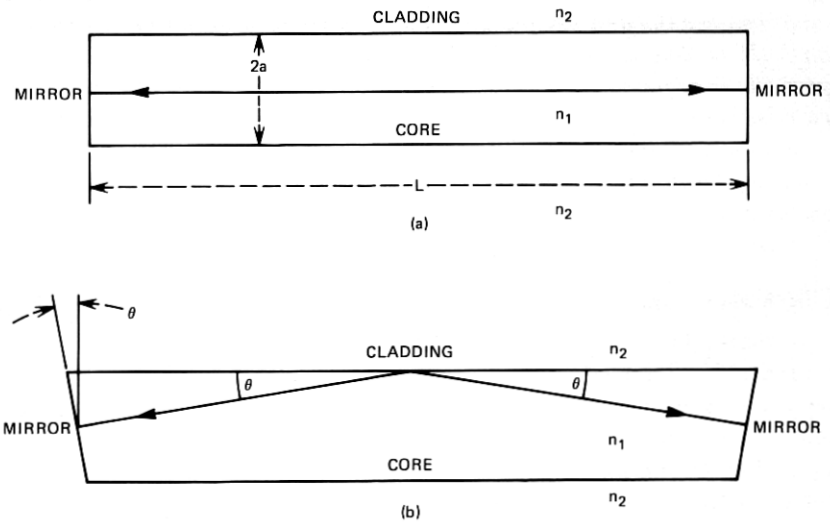

Fig. 1—Schematic of the fiber laser with (a) perpendicular mirrors and (b) tilted mirrors.

couples the perfect modes together. Coupling among the guided modes does not introduce losses by itself. However, the perfect modes of the fiber suffer losses individually (in the absence of coupling). These losses are either caused by dissipative mechanisms in the fiber core or in its cladding, or they may be caused by fiber imperfections on a scale different from those that couple the guided modes. We may assume that imperfections with Fourier components of high spatial frequencies couple each ideal fiber mode to the radiation field outside the fiber and act as a loss mechanism. In addition, there will probably be imperfections with large amplitudes but with low spatial frequencies that couple the ideal modes to each other.

In a companion paper[3] we discuss the influence of mode coupling on the losses of the normal modes of the fiber cavity. We found that coupling among these modes increases the cavity losses compared to the losses of the lowest-order ideal fiber mode because neighboring modes with higher losses take part in the superposition field that forms the cavity mode. We also found that strongly coupled modes result in a normal mode of the cavity whose loss is an average of the losses of the participating coupled modes. However, not all the ideal modes of the fiber take part in forming the normal mode of the fiber cavity. Modes whose individual losses (radiation losses as well as dissipation losses) are relatively higher than the coupling strength to neighboring guided modes do not take part in the loss-averaging process. Since the losses of the ideal fiber modes tend to increase in proportion to the square of their (compound) mode number, modes of high order are, of necessity, much lossier than modes of low order. On the other hand, it is expected that the coupling strength of neighboring guided modes decreases with mode number. Consequently, only modes with relatively low mode numbers participate in forming the normal modes of the cavity.

This theoretical expectation is confirmed by observation of laser radiation.[2] In fibers supporting a very large number of guided modes, only the modes of low order are excited as laser modes. Laser modes are identical with the normal modes of the resonant fiber cavity. It is thus clear that the loss of the normal mode of the laser (or fiber cavity) is an average value of the losses of the ideal modes that take part in forming the normal mode of the cavity. If only a very few fiber modes are taking part in forming the lasing mode, the loss (in the absence of pumping) of this cavity mode is simply the average loss of the few fiber modes that are effectively coupled to each other. In the presence of coupling among the guided modes, the loss of the resulting laser mode is thus somewhat higher than the loss coefficient of the fiber mode of lowest order, but mode coupling, even if strong

for the lowest-order fiber mode and its neighbor, does not increase the loss of the laser mode dramatically. The example studied in Ref. 3 suggests that the loss of the laser mode may be at most an order of magnitude higher than the loss of the fiber mode of lowest order. We found, furthermore, that two modes with propagation constants β_1 and β_2 can couple effectively only if the relation $\beta_1 - \beta_2 = 2n\pi/L$ holds to an accuracy on the order of $|\alpha_1 - \alpha_2|$, where α indicates the loss coefficient, n is an integer, and $L/2$ is the resonator length.

So far, we have assumed that the mirrors at the end of the fiber resonator are perfectly perpendicular to the fiber axis. Mirror tilt can be taken into account in the following way. Consider a light ray that propagates parallel to the fiber axis and strikes the tilted mirror of the resonator. After reflection, the ray impinges on the fiber wall at an angle that is twice the angle of the mirror tilt. Because scattering losses are proportional to the square of the angle between the incident ray and the fiber wall, it is clear that this ray, which originally traveled parallel to the fiber axis, suffers relatively high scattering loss. On the other hand, a ray that strikes the tilted mirror at normal incidence will strike the fiber wall at the mirror tilt angle shown in Fig. 1b. Such a ray suffers less scattering loss. In fact, it would appear that the mirror tilt angle is the minimum angle at which rays passing back and forth through the cavity may strike the fiber wall. It is not obvious that there should be a ray path that closes on itself and still impinges at the tilted mirror at normal incidence. But the normal mode of a resonator has the tendency to minimize its losses. It will thus be composed of rays that make the lowest possible angle with the rough fiber walls. Consequently, we shall assume that the field in the resonator strikes the fiber wall at the mirror tilt angle. Instead of computing mode losses, we use the scattering losses of waves impinging on the rough dielectric interface at the mirror tilt angle to calculate the loss of a cavity with tilted mirrors. If both mirrors are tilted differently, the larger of the two angles should be used.

We limit our discussion to fibers whose diameter is much larger than the wavelength of the radiation inside the fiber core. This assumption permits us to use a pseudo-plane-wave analysis. For simplicity, it is furthermore assumed that the refractive index difference between core and cladding material is so slight that reflectivity differences caused by polarization can be ignored; TE and TM modes thus have the same losses. When we violate this assumption in some of our examples, it should be remembered that our loss values apply to TE polarization.

Several types of wall roughness will be considered. The simplest imperfection is a sinusoidal variation of the fiber radius. A more com-

plicated wall distortion preserves the circular shape of the fiber but allows the diameter to vary randomly as a function of the longitudinal z coordinate. Finally, we consider a type of wall roughness that assumes that the Fourier spectrum of the wall distortion function is constant over all spatial frequencies of interest and that variations occur in both dimensions on the fiber surface with certain short correlation lengths. Scattering losses are expressed as functions of the amplitudes of the sinusoidal distortion or the variance and correlation lengths of the random distortion functions. Mode losses in the fiber and losses in the fiber cavity with tilted mirrors are considered for the case of scattering losses and the case of losses introduced by the lossy cladding.

We find that cladding losses do not have a large influence on the wave loss in the fiber core, but scattering losses can be very serious if the amplitude of the wall roughness approaches the wavelength of the radiation.

Spherically curved mirrors could reduce the losses of fiber lasers with larger diameter if they reduce the field intensity at the fiber wall. However, this loss reduction would work only for perfectly straight fibers with perpendicular mirrors and very large radii. Our estimates of fiber losses associated with tilted plane mirrors are equally valid for fiber cavities with tilted curved mirrors if the tilt angle is large enough. For straight fibers with perpendicular but curved mirrors, our loss results can be regarded as an upper limit. It should also be clear that mirror tilt can be translated into an abrupt tilt of the fiber axis.

The analysis presented in this paper was performed to provide insight into the tolerance requirements of Nd-YAG fiber lasers.[2] Our numerical examples are thus geared to the parameters of this laser. The intrinsic losses of the fiber laser are on the order of 10^{-3} cm^{-1} so that additional losses caused by fiber irregularities or a lossy cladding should remain below this value.

Exact loss formulas may be expressed in terms of Bessel functions so that their numerical evaluation becomes tedious. For this reason, we are here deriving simplified formulas that allow reasonable order-of-magnitude estimates to be readily calculated with the help of a simple pocket calculator. Such handy approximations are often more useful than the formidable exact formulas and serve the purpose of providing insight into the relevant variables of the problem. All our loss formulas are immediately applicable to optical fibers that support many modes. Their application to the fiber laser is straightforward if we can be sure that there is no additional fiber irregularity with low spatial frequency coupling the guided modes among each other. However, even if mode coupling exists, it is known from theoretical[3]

and experimental[2] evidence that only modes of very low order participate in the lasing process. This information allows us to use the fiber loss results for the laser if we keep in mind that the loss prediction of the fiber mode of lowest order may somewhat underestimate the laser losses. For this reason, we base our discussion of laser losses on the mode with compound mode number $M = 5$. This loss estimate for the laser may, in fact, be pessimistic, but it provides the correct order of magnitude of the loss coefficient that may be used to derive tolerance requirements for the fiber laser.

II. PLANE WAVE SCATTERING AT A PLANE INTERFACE

We base our loss analysis on the results of plane wave scattering at the rough planar interface between two dielectric media, as sketched in Fig. 2. Our analysis uses the theory of coupled modes. In this analysis, the incident plane wave is coupled to the continuum of modes of a medium that is divided into two half-spaces with a plane interface. The coupled mode theory is described in Ref. 4.

To first-order perturbation theory, the scattered power is computed as follows. First, we determine the amplitudes $c_j(\sigma_x, \sigma_y)$ of the continuum modes that are excited by the incident plane wave interacting with the rough interface

$$c_j(\sigma_x, \sigma_y) = \int_{-(L_y/2)}^{L_y/2} dy \int_0^{L_z} K_{j\sigma i} f(y, z) dz, \tag{1}$$

where the continuous variables σ_x and σ_y label the continuum modes, $K_{j\sigma i}$ is the coupling coefficient between incident wave and continuum modes, and β_i and β_σ are the propagation constants (z components of the propagation vectors) of incident and scattered (continuum) waves.

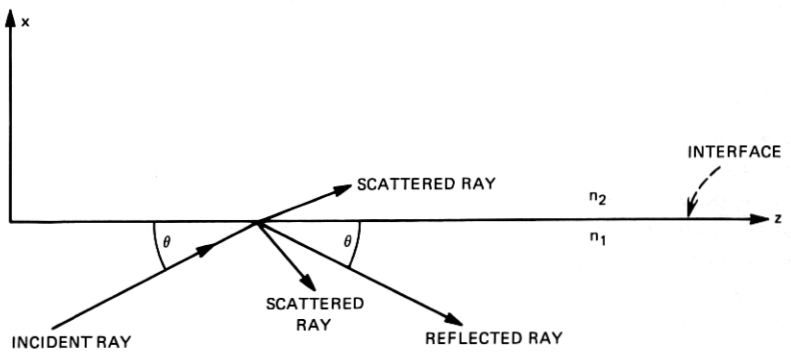

Fig. 2—Plane wave scattering at a plane, rough interface between two dielectric media with refractive indices n_1 and n_2. The y axis is directed perpendicular to the plane of the figure.

It is assumed that the rough surface with distortion function $f(y, z)$ extends only over an area L_yL_z in the y and z directions while the remainder of the infinite interface is perfectly flat. The coupling coefficient is defined as[4]

$$K_{j\sigma i} = \frac{\omega \epsilon_0}{4iP} (n_1^2 - n_2^2)[\mathbf{\mathcal{E}}^*_{\sigma_x,\sigma_y j} \cdot \mathbf{E}_i]_{x=0}. \tag{2}$$

In this formula, ω designates the angular frequency of the light waves, ϵ_0 is the dielectric permittivity, $\mathbf{E}_i$ is the electric vector of the incident and specularly reflected and transmitted waves of the perfect interface, while $\mathbf{\mathcal{E}}_{\sigma_x,\sigma_y j}$ indicates the electric field vector of the continuum mode. Label j designates the different types of continuum modes whose field expressions are given in the appendix and P in (2) is a power normalizing factor. The scattered power can now be calculated with the help of the formula[4]

$$P_{sc} = P \sum_j \iint_S |c_j(\sigma_x, \sigma_y)|^2 d\sigma_x d\sigma_y. \tag{3}$$

The summation extends over the different types of continuum modes, while the integration over the area S in the space σ_x, σ_y extends only over propagating continuum modes.

With the help of the mode fields listed in the appendix, we derive the following expressions for the scattered power. For a sinusoidal corrugation of the surface

$$f(y, z) = b \sin \Omega z, \tag{4}$$

we find

$$P_{sc} = \frac{b^2 S_z \kappa^2 k (n_1^2 - n_2^2) L_z L_y}{\beta_i (n_1 \sin \phi_1 + n_2 \sin \phi_2)}. \tag{5}$$

Here b is the amplitude of the sinusoidal deflection, S_z is the z component of the Poynting vector of the incident plane wave, and κ and β_i are, respectively, the x and z components of the propagation vector of the incident plane wave in the medium with index n_1 whose magnitude is $n_1 k$. For sinusoidal corrugation, the scattered plane waves are emitted in definite directions whose angles are defined by[4]

$$\cos \phi_1 = \frac{\beta_i - \Omega}{n_1 k} \tag{6}$$

in medium 1 and by

$$\cos \phi_2 = \frac{\beta_i - \Omega}{n_2 k} \tag{7}$$

in medium 2.

Next we list the scattering formula for scattering from a random corrugation. There is no variation of the surface in the y direction,

but the variation in the z direction with variance $\bar{\sigma}^2$ is random with a correlation length D_z that is much shorter than the wavelength of light. The total amount of scattered power from an area L_yL_z is

$$P_{sc} = \frac{4}{n_1} L_yL_zS_zD_z\bar{\sigma}^2\kappa^2k(n_1^2 - n_2^2)G_1\left(\frac{n_1}{n_2}\right), \tag{8}$$

with

$$G_1\left(\frac{n_1}{n_2}\right) = \frac{\sqrt{(n_1^2/n_2^2) - 1} - \frac{\pi}{2} + (n_1^2/n_2^2)\arcsin(n_2/n_1)}{\pi[(n_1^2/n_2^2) - 1]}$$
$$\approx 0.7162(n_2/n_1) - 0.6830(n_2/n_1)^2 + 0.4312(n_2/n_1)^3. \tag{9}$$

The polynomial was obtained as an empirical approximation of this function. Each component of the Fourier decomposition of the rough surface gives rise to two plane waves, one emitted into medium 1 and the other into medium 2. The directions of the two waves are related by Snell's law. If the angle (measured with respect to the surface) of the wave in medium 1, with the larger refractive index n_1, becomes so small that the angle of the wave in medium 2 becomes imaginary, no wave can escape into medium 2; but there is still a wave emitted into medium 1. Equation (8) contains the large-angle contributions from waves emitted into both media. However, at small scattering angles where the wave in medium 2 disappears, the scattered wave in medium 1 corresponds to a guided mode in a situation where medium 1 is the core of a fiber. Power scattered into guided mode directions is not lost, but becomes part of the "new" normal mode that establishes itself in the distorted fiber and is not included in (8).

Finally, we list the expression for the total scattered power when the interface is rough in y and z dimensions. The correlation length (much shorter than the wavelength) of the distortion in y direction is D_y,

$$P_{sc} = \frac{4}{\pi} L_yL_zD_yD_z\bar{\sigma}^2S_z\kappa^2k^2(n_1^2 - n_2^2)G_2\left(\frac{n_1}{n_2}\right). \tag{10}$$

In the previous two cases, radiation was escaping only in the x, z plane. In the case of a truly random surface distortion, radiation escapes isotropically in all directions. When we apply our present results to the case of fiber scattering, we want to distinguish between two types of radiation. Any ray direction not associated with a guided mode belongs to either a refracting or a tunneling leaky wave. Refracting leaky waves leave the fiber core because they impinge on the fiber boundary at an angle that cannot be contained inside the fiber by total internal reflection. Tunneling leaky waves consist of rays that should be trapped inside the fiber core by means of total internal

reflection.[5,6] However, tunneling leaky waves lose power by a mechanism that causes energy to tunnel through an evanescent wave region outside the fiber core to an external caustic from which they can escape. Refracting leaky rays are very lossy and can be considered radiative power. Tunneling leaky rays may have very low losses in fibers with large core diameters and may well be part of the "new" normal mode of the fiber cavity. It is thus desirable to be able to distinguish between power scattering into these two types of leaky rays. This distinction is made in the factor $G_2(n_1/n_2)$ appearing in (10). We write

$$G_2 = G_{2r} + G_{2t}. \tag{11}$$

G_{2r} incorporates only loss to refracting leaky rays, that is, rays scattered in those directions that, in a fiber, correspond to refracting leaky waves. G_{2t} incorporates the contribution from those scattering directions that, in a fiber, would correspond to tunneling leaky rays. Both expressions could be represented in closed form but, since the closed form formulas would be too unwieldy, we prefer to list them in the form of integrals:

$$G_{2r}\left(\frac{n_1}{n_2}\right) = \int_{\sqrt{1-(n_2^2/n_1^2)}}^{1} \frac{v(1-v^2) + 2v^2\sqrt{v^2 - [1-(n_2^2/n_1^2)]}}{(n_2^2/n_1^2)v + \sqrt{v^2 - [1-(n_2^2/n_1^2)]}}\, dv$$
$$\approx 0.2666(n_2/n_1) - 0.05359(n_2/n_1)^2 + 0.3990(n_2/n_1)^3 \tag{12}$$

and

$$G_{2t} = \frac{1}{3}\sqrt{1-(n_2^2/n_1^2)} - \frac{n_2}{3\pi n_1[1-(n_2^2/n_1^2)]}$$
$$\times \int_{(n_2/n_1)^2}^{1} \frac{\sqrt{1-v}}{v\sqrt{v-(n_2^2/n_1^2)}}[2v + 1 - 3(n_2^2/n_1^2)]dv \tag{13a}$$

$$G_2 \approx 0.1364(n_2/n_1) + 0.7926(n_2/n_1)^2 - 0.2592(n_2/n_1).^3 \tag{13b}$$

The polynomials are again empirical approximations. The functions G_1, G_{2r}, and $G_2 = G_{2r} + G_{2t}$ are plotted in Fig. 3. As a matter of curiosity, we note that, disregarding the differences between functions G_1 and G_2, (8) and (10) become identical if we set the correlations length in the y direction equal to

$$D_y = \frac{\pi}{n_1 k} = \frac{\lambda_0}{2n_1}. \tag{14}$$

Of course, this is a purely formal relationship, since (10) does not apply for a correlation length on the order of the wavelength.

III. LOSS DUE TO POWER DISSIPATION IN MEDIUM 2

In preparation for computing the fiber losses caused by a lossy jacket, we consider the plane wave reflection problem shown in Fig. 2 when

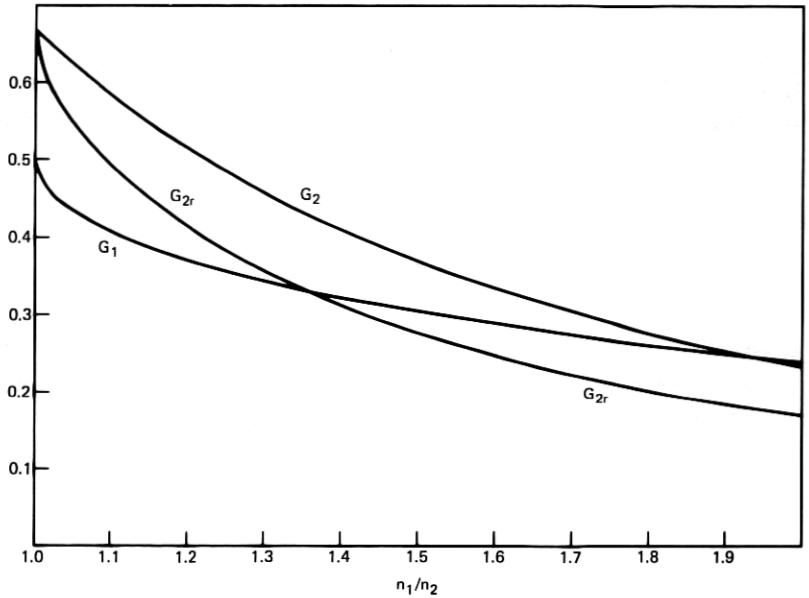

Fig. 3—The functions G_1, G_2, and G_{2r} defined by (9) and (11) through (13) plotted versus n_1/n_2.

n_1 is lossless and the interface is perfectly plane, but medium 2 is lossy. The reflection coefficient for total internal reflection from the plane interface is expressed by the formula[7]

$$r = \frac{\kappa + i\gamma}{\kappa - i\gamma}, \tag{15}$$

with

$$\kappa = \sqrt{n_1^2 k^2 - \beta_i^2} \tag{16}$$

and

$$\gamma = \sqrt{\beta_i^2 - n_2^2 k^2}. \tag{17}$$

Using

$$n_2 = n_{2r} - in_{2i} \tag{18}$$

and the amplitude loss coefficient for plane wave propagation in medium 2,

$$\alpha_2 = n_{2i} k, \tag{19}$$

we obtain from (15), (17), and (18)

$$R = |r|^2 \approx 1 - \frac{4\alpha_2 n_{2r} \kappa}{(n_1^2 - n_2^2)^{\frac{1}{2}} k^2}. \tag{20}$$

We have assumed that $n_{2i} \ll n_{2r}$ and used $\gamma^2 = (n_1^2 - n_{2r}^2)k^2$, an approximation that holds for incident waves whose angle (with respect

to the interface) is far below the critical angle. When we apply our results to optical fibers, this assumption means that we limit ourselves to modes far from cutoff. The amount of dissipated power in an area L_yL_z is now

$$P_d = L_yL_zS_x(1 - R). \tag{21}$$

S_x is the x component of the Poynting vector. We use the relation $S_x = (\kappa/\beta_i)S_z$ and obtain, from (20) and (21),

$$P_d = \frac{2(2\alpha_2)n_2L_yL_zS_z\kappa^2}{n_1(n_1^2 - n_2^2)^{\frac{1}{2}}k^3}. \tag{22}$$

The real part of the refractive index has again been replaced by the symbol n_2, and we used the approximation $\beta_i = n_1k$.

IV. APPLICATION TO MULTIMODE FIBERS

The guided-mode field in optical fibers can be approximated as[4]

$$E_y = AJ_\nu(\kappa r)\cos \nu\phi e^{-i\beta z}. \tag{23}$$

The power density flowing in the z direction is thus given by

$$S_z = \frac{1}{2}\frac{P}{\pi a^2}\cos^2 \nu\phi, \tag{24}$$

where P is the total power carried by the guided mode. Since the fiber radius is a, we obtain the power density $P/(\pi a^2)$. The factor $\frac{1}{2}$ appearing in (24) accounts for the fact that half the total power is carried by a wave traveling toward the core boundary while the other half travels away from the boundary after reflection. The factor $\cos^2 \nu\phi$ follows in an obvious manner from (23). Averaging over the entire circumference of the fiber, we obtain

$$\bar{S}_z = \frac{1}{4}\frac{P}{\pi a^2}. \tag{25}$$

The mode losses are now obtained from the plane wave formulas of the last two sections by identifying $L_y = 2\pi a$, replacing S_z with $\bar{S}_z$ of (25) and using the formula (for heat losses, P_{sc} is replaced by P_d)

$$2\alpha = \frac{P_{sc}}{L_zP}. \tag{26}$$

We can thus immediately compile the following list of power-loss coefficients for the various fiber loss mechanisms.

Sinusoidal radius variation of amplitude b:

$$2\alpha = \frac{b^2\kappa^2(n_1^2 - n_2^2)}{2an_1(n_1 \sin \phi_1 + n_2 \sin \phi_2)}. \tag{27}$$

The angles ϕ_1 and ϕ_2 are defined by (6) and (7).

Random radius variation with correlation length D_z and variance $\bar{\sigma}^2$:

$$2\alpha = \frac{2}{n_1 a} D_z \bar{\sigma}^2 \kappa^2 k (n_1^2 - n_2^2) G_1\left(\frac{n_1}{n_2}\right). \tag{28}$$

Random surface variation with correlation length D_ϕ (formerly called D_y) in the ϕ direction and D_z in the z direction and variance $\bar{\sigma}^2$:

$$2\alpha = \frac{2}{\pi a} D_\phi D_z \bar{\sigma}^2 \kappa^2 k^2 (n_1^2 - n_2^2) G_2\left(\frac{n_1}{n_2}\right). \tag{29}$$

Functions G_1, G_2, and G_{2r} are plotted in Fig. 3. Whether G_2 or G_{2r} is to be used depends on the length and size of the fiber. If tunneling leaky modes are only slightly attenuated in the length of fiber under consideration and can be regarded as guided modes, we must use G_{2r}; if tunneling leaky waves are very lossy, G_2 must be used; in intermediate cases, an average value may be appropriate. For a discussion of the losses of tunneling leaky waves, see Refs. 5 and 6. Finally, we list the power loss coefficient for a multimode fiber with lossy cladding (but lossless core) with cladding power-loss coefficients $2\alpha_2$:

$$2\alpha = \frac{(2\alpha_2) n_2 \kappa^2}{n_1 a (n_1^2 - n_2^2)^{\frac{1}{2}} k^3}. \tag{30}$$

It remains to specify the values of κ that must be inserted into formulas (27) through (30). In fibers supporting only one or very few guided modes, κ would have to be obtained as the solution of the eigenvalue equation. However, our formulas hold only for large fibers supporting many modes that are mostly far from cutoff. In this case, it is possible to approximate κ as[4*]

$$\kappa = \frac{\pi}{2a}(M - \tfrac{1}{2}). \tag{31}$$

The compound mode number M is a combination of the azimuthal mode number ν and the radial mode number μ,

$$M = \nu + 2\mu = 2, 3, 4, \cdots. \tag{32}$$

If we are interested in the losses of a fiber cavity with tilted mirrors, Fig. 1b suggests that we use the expression

$$\kappa = n_1 k \sin\theta. \tag{33}$$

In this case, the field impinges on the fiber wall not at the natural mode angle applicable for perfectly straight fibers but at a larger angle θ that is imposed by the gross deformation of the fiber or mirror

* Eq. (31) holds for small values of ν. For large ν, we must replace $(\kappa a)^2 \to U^2 - \nu^2$ [see Ref. 4, p. 90, eq. (2.5–6)] and obtain U as the solution of $J_\nu(U) = 0$.

geometry. For fiber lasers, it seems reasonable to associate θ with the mirror tilt angle. For fibers with abrupt tilts, θ would be the fiber tilt angle.

Our derivation of formulas for the fiber loss coefficients was based on the properties of plane wave interaction with a plane interface. It is thus clear that our equations are only approximately valid. In particular, they do not incorporate interference effects between directly scattered rays and rays that leave the fiber after repeated reflections inside the fiber core. Such effects are particularly pronounced for scattering from purely sinusoidal core radius variations because, in this case, the radiation leaves at a definite angle and may be enhanced or reduced by interference effects.[8] Our equations give an average over the maxima and minima of the loss fluctuations as a function of scattering angle. The formulas for scattering from random surface effects or heat losses in the cladding are more reliable because diffuse scattering causes radiation to escape in all directions and interference effects tend to cancel out and are unimportant in the case of power dissipation in the cladding. The formulas derived here are handy order-of-magnitude approximations of the precise expressions containing Bessel functions.[4,8]

V. DISCUSSION AND NUMERICAL RESULTS

In this section, we present loss coefficients in graphic form. We begin with a fiber with sinusoidal core radius variations of amplitude b and spatial frequency Ω. Scattering losses occur only if the radiation can escape into the cladding. The spatial frequency range that results in scattering losses is thus obtained from (7) as

$$(n_1 - n_2)k < \Omega < (n_1 + n_2)k, \tag{34}$$

where we have assumed that $\beta_i \approx n_1 k$. If we introduce the length of the spatial period as $\Lambda = 2\pi/\Omega$, we obtain from (34) and $k = 2\pi/\lambda_0$

$$\frac{\lambda_0}{n_1 - n_2} > \Lambda > \frac{\lambda_0}{n_1 + n_2}. \tag{35}$$

These formulas apply, of course, also to the spatial frequency range that contributes to random scattering, discussed below.

Figure 4 shows curves plotted from (27). On the horizontal axis, we have plotted the normalized spatial frequency $\Omega/n_1 k$ and also the scattering angle Φ_2 at which the radiation escapes into medium 2. Beyond $\Omega/n_1 k = 1$, the curves form the mirror image of the section shown in the figure and were consequently omitted. Figure 4 was computed for YAG with $n_1 = 1.8$ and $n_2 = 1$. The parameter of the curves in Fig. 4 is the compound mode number M defined by (32).

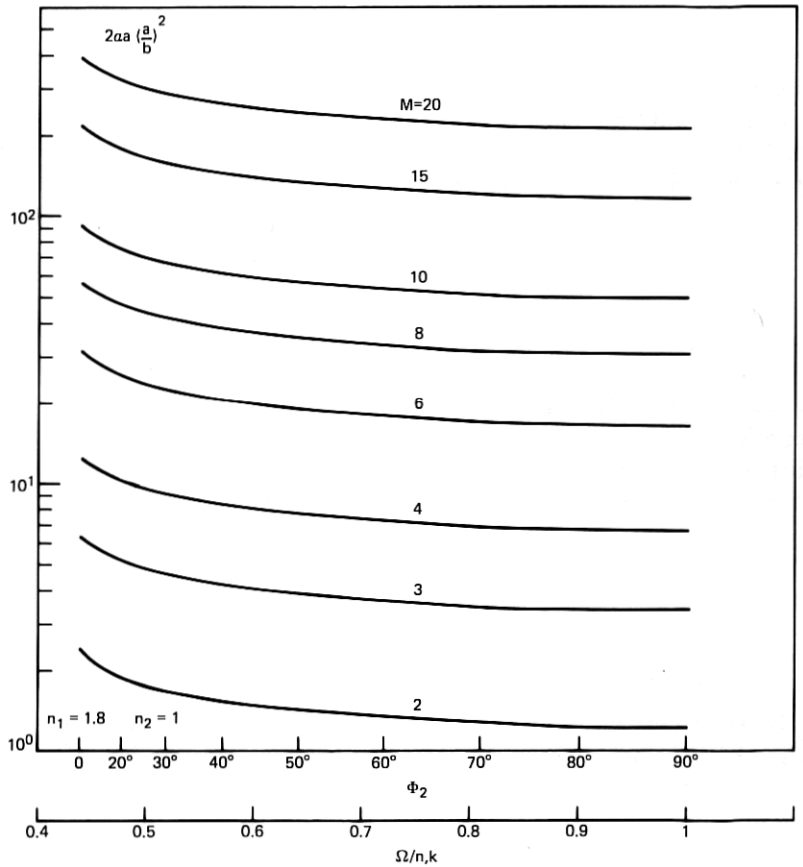

Fig. 4—Normalized scattering loss coefficient for a cavity with perpendicular mirrors (relative to the fiber axis) and sinusoidal core radius variation of amplitude b and spatial frequency Ω. M is the compound mode number. For this set of curves, $n_1 = 1.8$, $n_2 = 1.0$.

To obtain a feeling for the magnitude of the normalized loss coefficient and for the tolerance requirements, we assume that the fiber resonator has an inherent loss of $2\alpha = 10^{-3}$ cm^{-1} and a core radius of $a = 40$ μm. Scattering loss begins to be of concern if its magnitude equals the already existing cavity losses. Allowing for the possibility that a few fiber modes of low order are tightly coupled by some fiber deformation of large amplitude but with a spatial frequency below range (34), we use an average value of $2\alpha a^3/b^2 = 10$. If we are willing to tolerate a loss of $2\alpha = 10^{-3}$ cm^{-1} for $a = 40$ μm, we find as the maximum permissible ripple amplitude the value $b = 2.5 \times 10^{-2}$ μm.

Figure 5 shows curves that are similar to Fig. 4 except that we have

assumed that the YAG fiber now carries a cladding with refractive index $n_2 = 1.5$. It is apparent that the cladding causes a reduction of the scattering loss by roughly a factor of 2 so that we can now tolerate a ripple amplitude that is larger by $\sqrt{2}$.

Figure 6 still describes a cavity with a fiber with sinusoidal core radius variation, but in this case we have assumed that the mirrors are tilted by an angle θ. The tilt of the mirrors causes the field inside the cavity to impinge on the fiber wall at an angle that is roughly equal to the tilt angle. It is interesting to consider the intrinsic mode angle to obtain a feeling for the severity of tilt angles introduced externally.

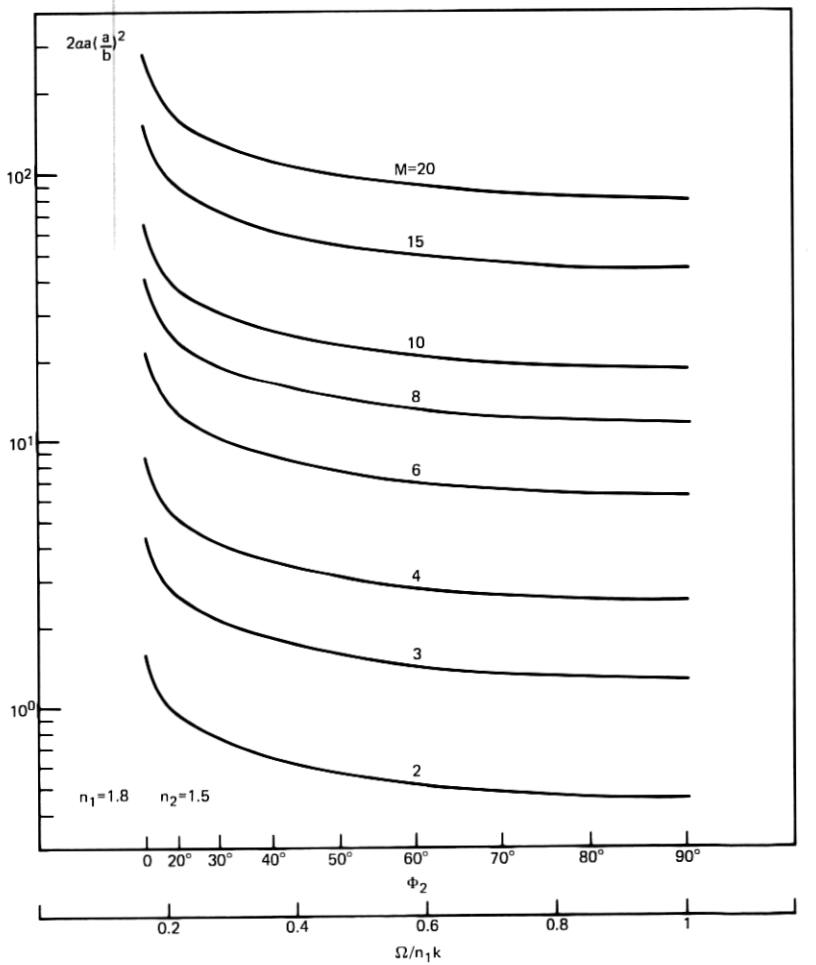

Fig. 5—Same as Fig. 4 but with $n_2 = 1.5$.

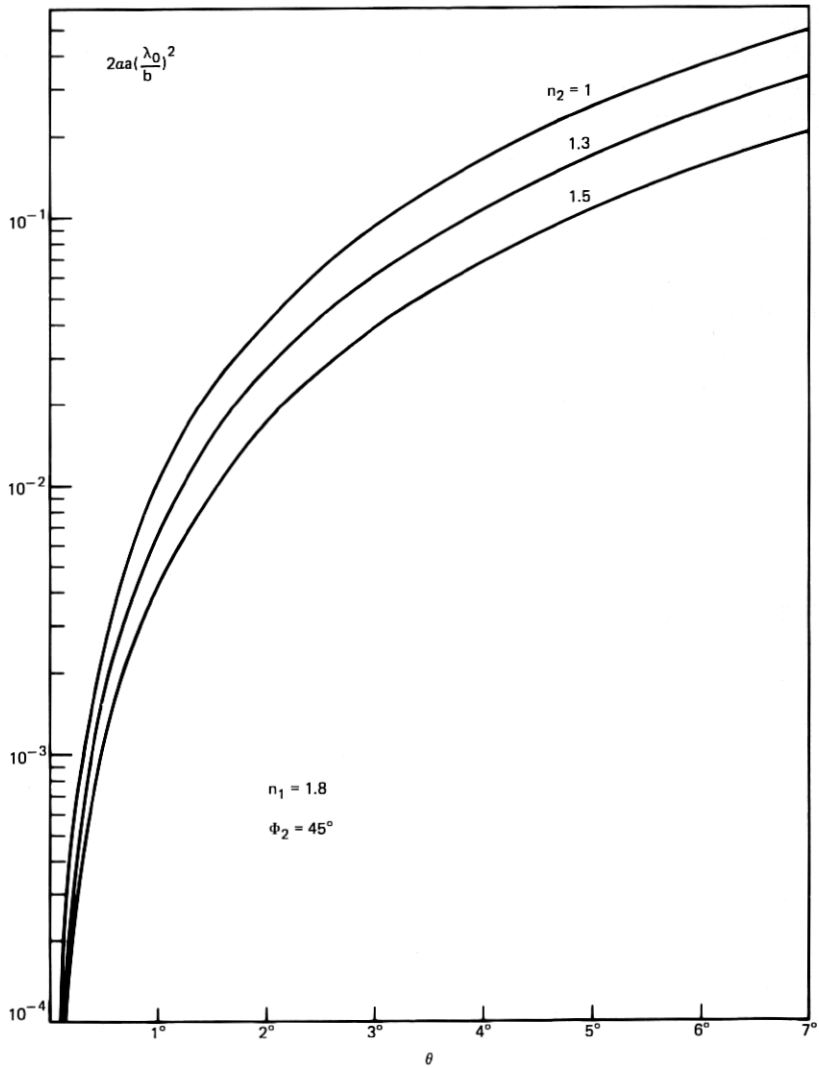

Fig. 6—Normalized scattering loss coefficient for a cavity with tilted mirrors, tilt angle θ, and sinusoidal core radius variation of amplitude b and spatial frequency Ω ($n_1 = 1.8$ and $\Phi_2 = 45$ degrees).

By equating (31) and (33), we find for the mode angle

$$\theta_M = \arcsin\left(\frac{\pi(M - \frac{1}{2})}{2n_1 ka}\right). \tag{36}$$

For $a = 40$ μm, $\lambda_0 = 1.06$ μm, and $n_1 = 1.8$, we find $\theta_M = 0.32$ degree for the fiber mode of lowest order, with $M = 2$ and $\theta_M = 2$

degrees for $M = 10$. We have assumed that mirror tilt can be controlled fairly accurately and extended our curves only to $\theta = 7$ degrees. It is now more natural to normalize the loss coefficient as $2\alpha a(\lambda_0/b)^2$. At a tilt angle of $\theta = 5$ degrees, we may expect for $n_1/n_2 = 1.8$ the normalized loss $2\alpha a(\lambda_0/b)^2 = 0.25$ according to Fig. 6. With $2\alpha = 10^{-3}$ cm^{-1}, $a = 40$ μm and $\lambda_0 = 1.06$ μm, we find the ripple amplitude $b = 4.2 \times 10^{-3}$ μm, which is a more stringent tolerance requirement than the value found for straight mirrors.

Next we consider a cavity with a fiber with randomly varying core radius. The case of a cavity with perpendicular mirrors is plotted from (28) and (9) in Fig. 7. It is assumed that the rms amplitude of the random core radius variation is $\bar{\sigma}$ and that the correlation length D_z is much shorter than the wavelength of light. If the cavity loss is an average value of fiber mode losses corresponding to $M = 5$ in Fig. 7, we have $2\alpha a^3\lambda_0/D_z\bar{\sigma}^2 = 200$. With $a = 40$ μm and $2\alpha = 10^{-3}$ cm^{-1}, we obtain $D_z\bar{\sigma}^2 = 3.4 \times 10^{-5}$ μm^3. For want of more information, we assume that $\bar{\sigma} = D_z$, so that we have $D_z = \bar{\sigma} = 3.2 \times 10^{-2}$ μm. This

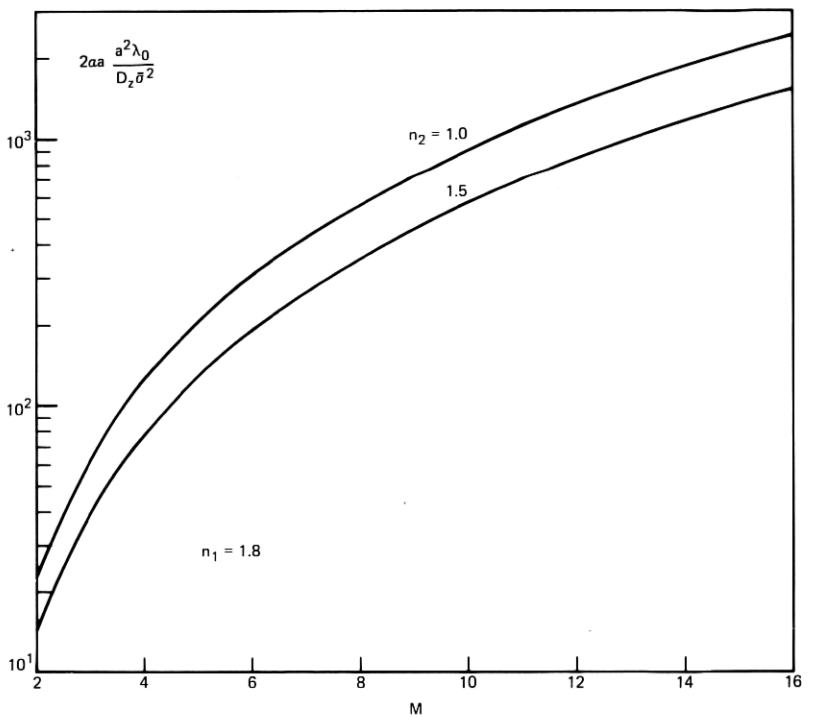

Fig. 7—Normalized scattering loss coefficient for a cavity with perpendicular mirrors and random core radius variations with variance $\bar{\sigma}^2$ and correlation length D_z. M is the compound mode number, $n_1 = 1.8$.

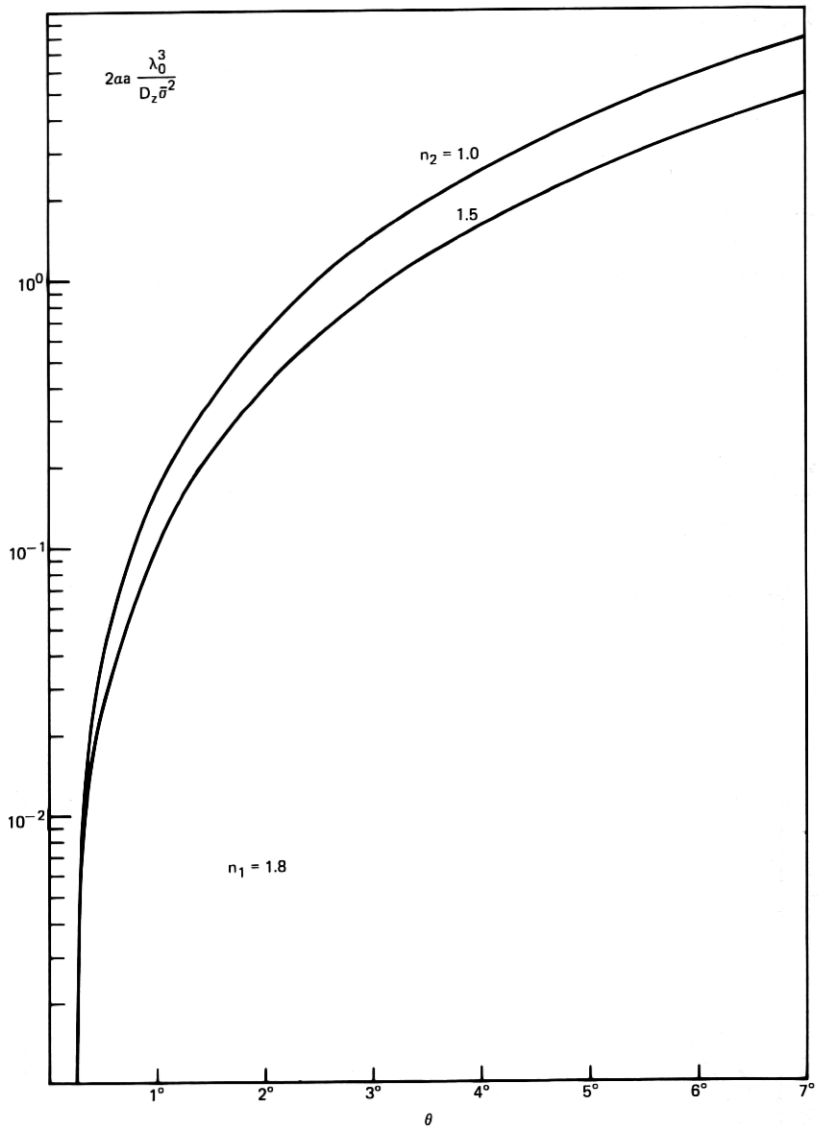

Fig. 8—Normalized scattering loss coefficient for a cavity with tilted mirrors, tilt angle θ, and random core radius variation for $n_1 = 1.8$.

value is quite comparable to the value $b = 2.5$ μm that we found in the case of a sinusoidal core radius variation.

Figure 8 gives the normalized scattering loss for a cavity with random core radius variation for the case of tilted mirrors. For $n_2 = 1$ and $\theta = 5$ degrees, we find from Fig. 8 $2\alpha a\lambda_0^3/D\bar{\sigma}^2 = 4$. With $a = 40$

μm, we obtain a loss of $2\alpha = 10^{-3}$ cm^{-1} for $D_z\bar{\sigma}^2 = 1.2 \times 10^{-6}$ μm^3 or $D_z = \bar{\sigma} = 1.1 \times 10^{-2}$ μm.

Figures 9 and 10 pertain to fibers with random core-cladding interface perturbations. Figure 9 describes a fiber cavity with perpendicular mirrors. At $M = 5$ we find, from Fig. 9, $2\alpha a^3\lambda_0^2/D_\phi D_z\bar{\sigma}^2 = 600$. With the usual values for loss, core radius, and light wavelength, we have $D_\Phi D_z\bar{\sigma}^2 = 1.2 \times 10^{-5}$ μm^4 or $D_\Phi = D_z = \bar{\sigma} = 5.9 \times 10^{-2}$ μm. If we let the two correlation lengths equal the rms variation of the interface, we find that the tolerance requirements are a little less stringent for a totally random surface compared to a surface that maintains its circular cross section and only allows the radius to vary along z.

Figure 10 shows the normalized loss coefficient for random core-cladding interface perturbations (in two dimensions) for a cavity with tilted mirrors. For a mirror tilt of $\theta = 5$ degrees, we obtain from Fig. 10 approximately $2\alpha a\lambda_0^4/D_\Phi D_z\bar{\sigma}^2 = 12$. With $a = 40$ μm, a loss of $2\alpha = 10^{-3}$ cm^{-1} is obtained for $D_\Phi D_z^{-2} = 4.2 \times 10^{-7}$ μm^4 or $D_\Phi = D_z = \bar{\sigma} = 2.5 \times 10^{-2}$ μm.

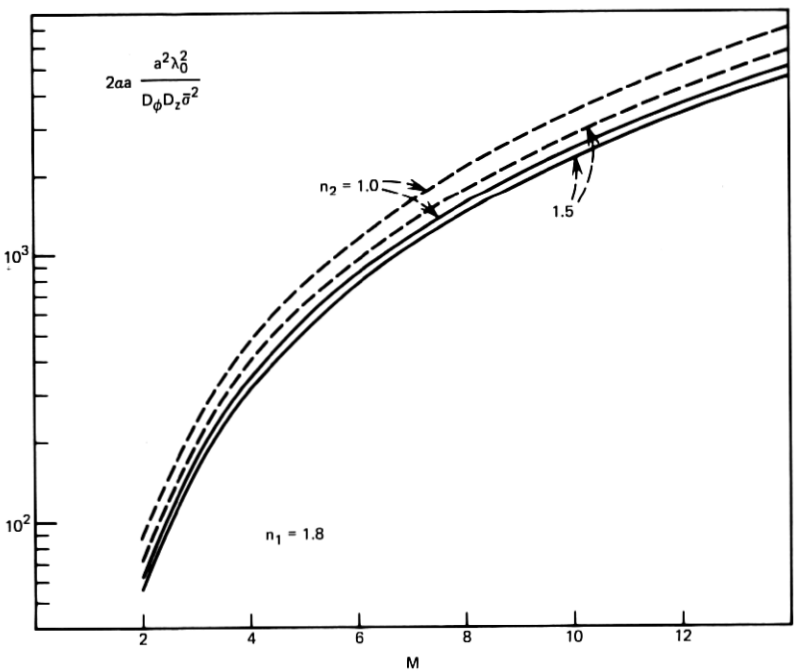

Fig. 9—Normalized scattering loss coefficient for a cavity with perpendicular mirrors and random core-cladding interface perturbations with correlation length D_ϕ in azimuthal direction, D_z in z direction, and variance $\bar{\sigma}^2$. The solid lines apply to a fiber whose tunneling leaky waves may be regarded as lossless guided waves; the dotted lines belong to the case in which tunneling leaky waves are so lossy that they cannot be regarded as guided waves. M is the compound mode number, $n_1 = 1.8$.

The remaining figures, 11 and 12, describe the normalized loss coefficient for a geometrically perfect fiber core surrounded by a lossy cladding. The power loss coefficient of a plane wave traveling in the material of the cladding is $2\alpha_2$. Figure 11 gives the mode losses of the fiber as a function of the normalized frequency parameter

$$V = \frac{2\pi a}{\lambda_0} (n_1^2 - n_2^2)^{\frac{1}{2}}. \tag{37}$$

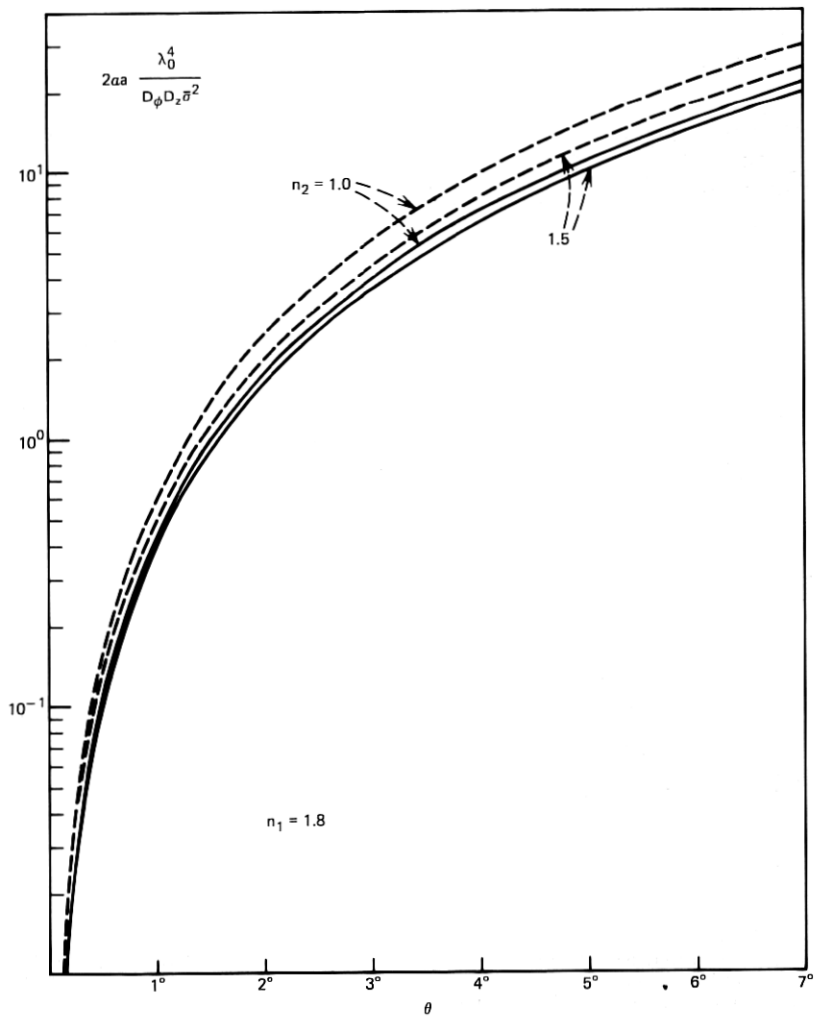

Fig. 10—Similar to Fig. 9 except that the cavity in this case has tilted mirrors with tilt angle θ.

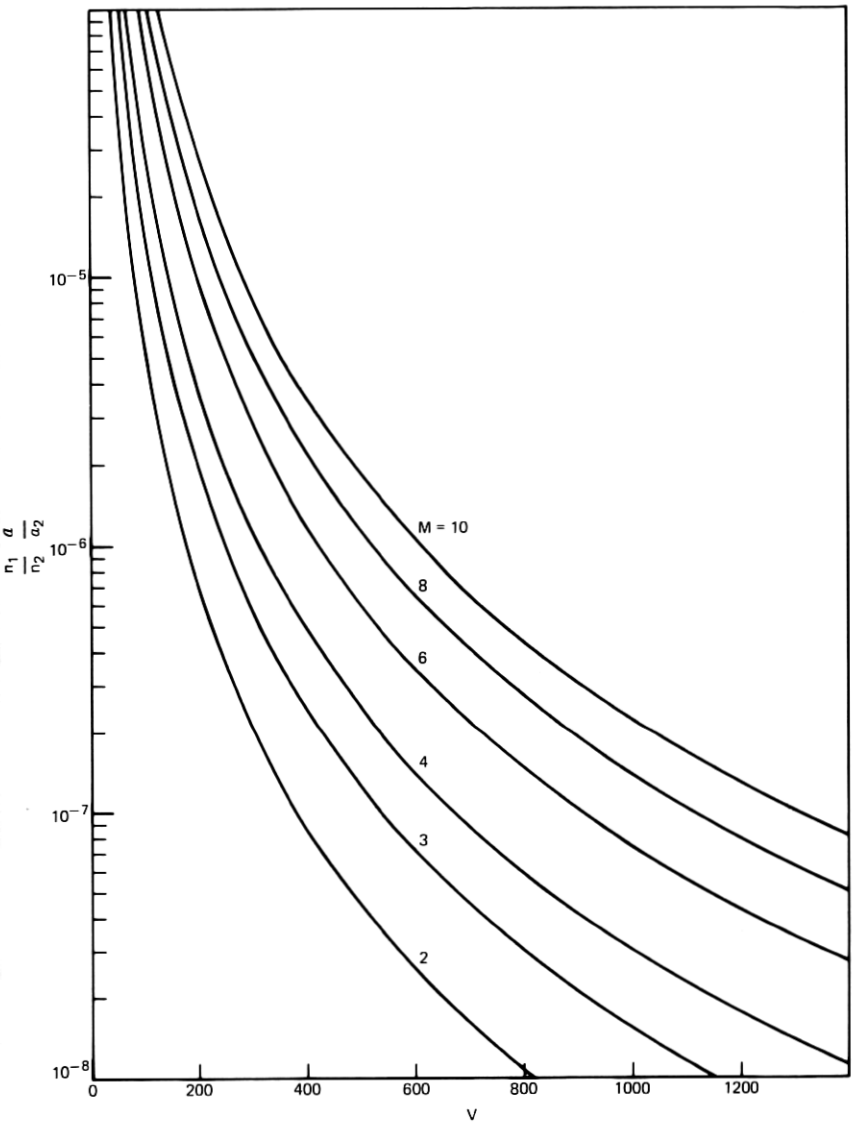

Fig. 11—Absorption loss coefficient of a fiber with lossy cladding (cladding loss coefficient α_2). This set of curves applies to the case of a cavity with perpendicular mirrors. The normalized frequency V is defined by (37).

For $\lambda_0 = 1.06$ μm, $a = 40$ μm, $n_1 = 1.8$, and $n_2 = 1$, we obtain $V = 355$ from (37). For $M = 5$, we obtain from Fig. 11 approximately $n_1\alpha_1/n_2\alpha_2 = 10^{-6}$. The mode losses are thus much less than

the cladding losses. For $2\alpha = 10^{-3}$ cm^{-1} and $n_1/n_2 = 1.8$, we could tolerate a cladding loss of $2\alpha_2 = 1.8 \times 10^3$ cm^{-1}. If we use $n_2 = 1.5$, we have $V = 236$ leading to $n_1\alpha/n_2\alpha_2 = 4 \times 10^{-6}$ at $M = 5$. With $n_1/n_2 = 1.2$, we can now tolerate $2\alpha_2 = 300$ cm^{-1}.

Figure 12 applies to a cavity with tilted mirrors and lossy jacket.

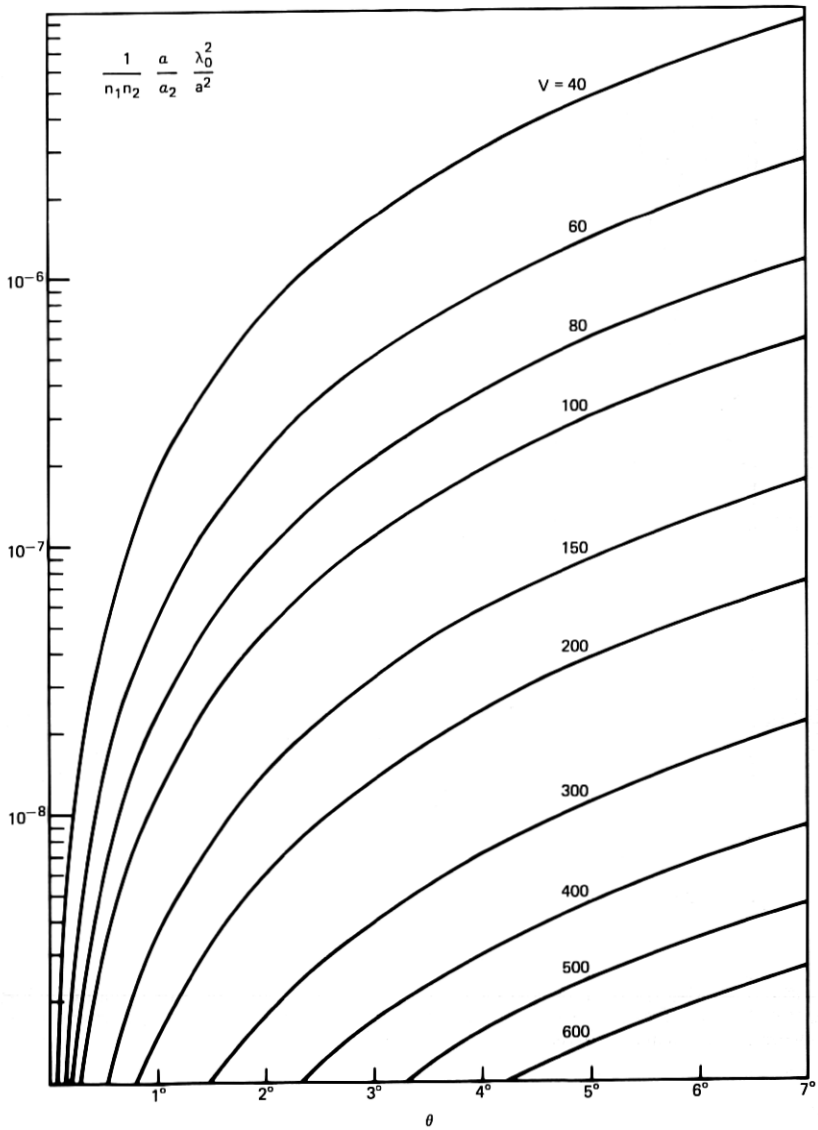

Fig. 12—Absorption loss coefficient of a fiber with lossy cladding (loss coefficient α_2). These curves apply to the case of a cavity with tilted mirrors, tilt angle θ.

Table I — Results of numerical evaluations of cladding losses. The cladding loss, $2\alpha_2$, gives rise to a mode loss of $2\alpha = 10^{-3}$ cm^{-1}

V	n_1/n_2	$2\alpha_2$	
		$M = 5, \quad \theta = 0$	$\theta = 5°$
355	1.8	1.8×10^3 cm^{-1}	56 cm^{-1}
236	1.2	300	10.4

For $\theta = 5$ degrees and $V = 355$, we find $\alpha\lambda_0^2(n_1 n_2 \alpha_2 a^2) = 7 \times 10^{-9}$. With $n_1 = 1.8$, $n_2 = 1$, $a = 40$ μm, and $2\alpha = 10^{-3}$ cm^{-1}, we can tolerate $2\alpha_2 = 56$ cm^{-1}. If $V = 236$ and $n_2 = 1.5$, we can tolerate $2\alpha_2 = 10.4$ cm^{-1}. These results are summarized in Table I.

VI. CONCLUSIONS

We have studied the losses of fibers and fiber resonators that are caused by perturbations of the core-cladding interface and by absorption losses of the cladding material. Formulas for the loss coefficient were derived by using plane wave techniques, and representative examples were displayed in the form of normalized curves. The theory presented here is not precise, and its application to practical cases is hampered by lack of knowledge of coupling among the guided modes. We have seen in a previous paper[3] that mode coupling tends to increase the cavity losses above the minimum value of the fiber mode of lowest order. However, the loss increase due to mode coupling results only in an average loss of a few of the lower-order modes that are coupled particularly tightly. We have thus concentrated on an average loss corresponding to mode $M = 5$ when we considered explicit loss values. Our results are useful to gain insight into the order of magnitude of fiber tolerances that must be maintained and into the amount of cladding losses that can be tolerated. We found that the tolerances of core-cladding interface perturbations are on the order of 0.01 μm, while cladding losses can be allowed to be as high as 10 cm^{-1} in the worst case of a cavity with mirrors tilted by 5 degrees, or as high as 300 cm^{-1} in the case of a cavity with perfectly perpendicular mirrors. Mirror losses were lumped in with the "background losses" of the cavity, which were assumed to be $2\alpha = 10^{-3}$ cm^{-1} in all the numerical examples we have considered. All curves independent of mirror tilt can be used to obtain the losses of optical fibers because they show plots of fiber mode losses without being tied to an application to fiber resonators.

VII. ACKNOWLEDGMENT

Many helpful discussions with J. Stone are gratefully acknowledged.

APPENDIX

For the calculation of scattering losses of a plane wave impinging on an irregular dielectric interface, we need to know the radiation modes of a space consisting of two dielectric media with refractive indices n_1 and n_2 separated by a plane interface. There are several types of such radiation modes. In each case, we list only the E_z and H_z components of their electric and magnetic fields, since all other field components follow from these longitudinal components by differentiation.[9] The time dependence of the modes is understood to be of the form

$$e^{i\omega t}. \tag{38}$$

We place our coordinate system so that the interface between the media with n_1 and n_2 lies in the y-z plane. We assume that $n_1 > n_2$ and let the medium with index n_2 be in the half space $x > 0$.

There are radiation modes whose fields decay exponentially in positive x direction for $x > 0$. These modes can be grouped further into modes with $E_x = 0$ and $H_x = 0$.

(i) Evanescent modes with $E_z = 0$:

$$\left.\begin{aligned} \mathcal{E}_z &= A_1 e^{-\Delta x} e^{-i(\sigma_y y + \beta z)} \\ \mathcal{H}_z &= i \frac{\beta \Delta}{\omega \mu_0 \sigma_y} A_1 e^{-\Delta x} e^{-i(\sigma_y y + \beta z)} \end{aligned}\right\} \quad \text{for} \quad x \geqq 0 \tag{39}$$

$$\left.\begin{aligned} \mathcal{E}_z &= A_1 \left(\cos \sigma_x x - i \frac{\Delta}{\sigma_x} \sin \sigma_x x \right) e^{-i(\sigma_y y + \beta z)} \\ \mathcal{H}_z &= i \frac{\beta \sigma_x}{\omega \mu_0 \sigma_y} A_1 \left[\sin \sigma_x x - \frac{\Delta}{\sigma_x} \cos \sigma_x x \right] e^{-i(\sigma_y y + \beta z)} \end{aligned}\right\} \quad \text{for} \quad x \leqq 0. \tag{40}$$

The parameters entering these equations are related by

$$n_1^2 k^2 = \sigma_x^2 + \sigma_y^2 + \beta^2 \tag{41}$$

and

$$n_2^2 k^2 = -\Delta^2 + \sigma_y^2 + \beta^2. \tag{42}$$

The fields are normalized with respect to a delta function,

$$\frac{1}{2} \int\int (\mathcal{E}_x \mathcal{H}_y^* - \mathcal{E}_y \mathcal{H}_x^*) dx dy = P \delta(\sigma_x - \sigma_x') \delta(\sigma_y - \sigma_y'), \tag{43}$$

so that we obtain for the amplitude coefficient

$$A_1^2 = \frac{2a^2 \omega \mu_0 \sigma_x^2 \sigma_y^2 P}{\pi^2 V^2 \beta (\beta^2 + \sigma_y^2)}, \tag{44}$$

with V defined by (37) and μ_0 indicating the magnetic permeability of vacuum.

(*ii*) Evanescent modes with $H_x = 0$:

$$\left.\begin{aligned} \mathcal{E}_z &= A_2 e^{-\Delta x} e^{-i(\sigma_y y+\beta z)} \\ \mathcal{H}_z &= i\frac{n_2^2 k^2 \sigma_y}{\omega\mu_0\beta\Delta} A_2 e^{-\Delta x} e^{-i(\sigma_y y+\beta z)} \end{aligned}\right\} \quad \text{for } x \geqq 0 \quad (45)$$

$$\left.\begin{aligned} \mathcal{E}_z &= A_2\left(\cos\sigma_x x + \frac{n_2^2}{n_1^2}\frac{\sigma_x}{\Delta}\sin\sigma_x x\right) e^{-i(\sigma_y y+\beta z)} \\ \mathcal{H}_z &= i\frac{n_2^2 k^2 \sigma_y}{\omega\mu_0\beta\Delta} A_2\left(\cos\sigma_x x - \frac{n_1^2}{n_2^2}\frac{\Delta}{\sigma_x}\sin\sigma_x x\right) e^{-i(\sigma_y y+\beta z)} \end{aligned}\right\} \quad \text{for } x \leqq 0. \quad (46)$$

Equations (41) and (42) still apply, and the amplitude coefficient is

$$A_2^2 = \frac{2\omega\mu_0 n_1^2 \sigma_x^2 \Delta^2 \beta P}{\pi^2 k^2 (n_2^4\sigma_x^2 + n_1^4\Delta^2)(\beta^2 + \sigma_y^2)}. \quad (47)$$

These first two types of modes are valid only in a limited range of σ_x and σ_y that is determined by the requirement that Δ, defined by (42), must be a positive real quantity.

(*iii*) Full standing wave modes with $E_x = 0$:

$$\left.\begin{aligned} \mathcal{E}_z &= A_{3j}(\cos\rho_x x + R_j \sin\rho_x x) e^{-i(\sigma_y y+\beta z)} \\ \mathcal{H}_z &= i\frac{\beta\rho_x}{\omega\mu_0\sigma_y} A_{3j}(\sin\rho_x x - R_j\cos\rho_x x) e^{-i(\sigma_y y+\beta z)} \end{aligned}\right\} \quad \text{for } x \geqq 0 \quad (48)$$

$$\left.\begin{aligned} \mathcal{E}_z &= A_{3j}\left(\cos\sigma_x x + \frac{\rho_x}{\sigma_x} R_j \sin\sigma_x x\right) e^{-i(\sigma_y y+\beta z)} \\ \mathcal{H}_z &= i\frac{\beta\sigma_x}{\omega\mu_0\sigma_y} A_{3j}\left(\sin\sigma_x x - \frac{\rho_x}{\sigma_x} R_j\cos\sigma_x x\right) e^{-i(\sigma_y y+\beta z)} \end{aligned}\right\} \quad \text{for } x \leqq 0. \quad (49)$$

Equation (41) applies in this case, too, but (42) is replaced by

$$n_2^2 k^2 = \rho_x^2 + \sigma_y^2 + \beta^2. \quad (50)$$

The coefficient R_j is arbitrary, but it is convenient to choose two values R_1 and R_2 so that the two resulting modes become mutually orthogonal. We choose for convenience

$$R_1 = 0 \quad (51)$$

and

$$R_2 = \infty. \quad (52)$$

The corresponding amplitude coefficients are

$$A_{31}^2 = \frac{2\sigma_x\sigma_y^2\omega\mu_0 P}{\pi^2\beta(\sigma_x + \rho_x)(\beta^2 + \sigma_y^2)} \quad (53)$$

and

$$R_2^2 A_{32}^2 = \frac{2\sigma_x^2\sigma_y^2\omega\mu_0 P}{\pi^2\beta\rho_x(\sigma_x + \rho_x)(\beta^2 + \sigma_y^2)}. \quad (54)$$

(*iv*) Full standing wave modes with $H_x = 0$:

$$\left.\begin{aligned} \mathcal{E}_z &= A_{4j}(\cos \rho_x x + S_j \sin \rho_x x)e^{-i(\sigma_y y+\beta z)} \\ \mathcal{H}_z &= -i\frac{\omega \epsilon_0 \sigma_y n_2^2}{\rho_x \beta} A_{4j}(\sin \rho_x x - S_j \cos \rho_x x)e^{-i(\sigma_y y+\beta z)} \end{aligned}\right\} \text{ for } x \geqq 0. \quad (55)$$

$$\left.\begin{aligned} \mathcal{E}_z &= A_{4j}\left(\cos \sigma_x x + \frac{\rho_x}{\sigma_x} S_j \sin \sigma_x x\right) e^{-i(\sigma_y y+\beta z)} \\ \mathcal{H}_z &= -i\frac{\omega \epsilon_0 \sigma_y n_1^2}{\sigma_x \beta} A_{4j}\left(\sin \sigma_x x - \frac{n_2^2}{n_1^2}\frac{\sigma_x}{\rho_x} S_j \cos \sigma_x x\right) e^{-i(\sigma_y y+\beta z)} \end{aligned}\right\} \text{ for } x \leqq 0. \quad (56)$$

Equations (41) and (50) determine the relations among the components of the propagation constant. The ranges of σ_x and σ_y are limited to the regions where ρ_x is real and positive. This remark applies also to case (*iii*).

Two sets of mutually orthogonal modes result if we choose

$$S_1 = 0 \quad (57)$$

and

$$S_2 = \infty. \quad (58)$$

The amplitude coefficients are

$$A_{41}^2 = \frac{2\rho_x \sigma_x^2 \sqrt{\mu_0/\epsilon_0}\beta P}{\pi^2 k(n_2^2\sigma_x + n_1^2\rho_x)(\beta^2 + \sigma_y^2)} \quad (59)$$

and

$$S_2^2 A_{42}^2 = \frac{2n_1^2 \sigma_x \rho_x^2 \sqrt{\mu_0/\epsilon_0}\beta P}{\pi^2 n_2^2 k(n_2^2\sigma_x + n_1^2\rho_x)(\beta^2 + \sigma_y^2)}. \quad (60)$$

ϵ_0 is the permittivity of vacuum.

REFERENCES

1. P. W. Smith, "A Waveguide Gas Laser," Appl. Phys. Lett., *19*, No. 5 (September 1971), pp. 132–134.
2. J. Stone, C. A. Burrus, A. G. Dentai, and B. I. Miller, "Nd:YAG Single-Crystal Fiber Laser: Room Temperature CW Operation Using A Single LED as an End Pump," Appl. Phys. Lett., *29*, No. 1 (July 1976), pp. 37–39.
3. D. Marcuse, "Steady-State Losses of Optical Fibers and Fiber Resonators," B.S.T.J., this issue, pp. 1445–1462.
4. D. Marcuse, *Theory of Dielectric Optical Waveguides*, New York: Academic Press, 1974.
5. A. W. Snyder and J. D. Love, "Tunneling Leaky Modes on Optical Waveguides," Opt. Commun., *12*, No. 3 (November 1974), pp. 326–328.
6. A. W. Snyder, "Leaky-Ray Theory of Optical Waveguides of Circular Cross Section," Appl. Phys., *4*, 1974, pp. 273–298.
7. D. Marcuse, *Light Transmission Optics*, New York: Van Nostrand Reinhold, 1972, p. 18, eq. (1.6-14).
8. D. Marcuse, "Radiation Losses of the HE_{11} Mode of a Fiber with Sinusoidally Perturbed Core Boundary," Appl. Opt., *14*, No. 12 (December 1975), pp. 3021–3025.
9. Ref. 7, pp. 12–13, eqs. (1.4-16) through (1.4-19).